A Novel 5G TDD Cellular System Proposal based on Multipath Division Multiple Access

Wei-Han Hsiao, Chia-Chi Huang

Department of Electrical and Computer Engineering, National Chiao Tung University, Hsinchu, Taiwan, ROC

whsiao.cm97g@g2.nctu.edu.tw, huangcc@faculty.nctu.edu.tw

***Abstract*—Evolving from the 3G and the 4G communication systems, the 5G system demands both high system capacity and high data rate. A novel time division duplexing (TDD) cellular system based on multipath division multiple access (MDMA) with massive antennas in millimeter wave band is proposed in this paper. The system is built on multipath division multiple access which is a method to use massive antennas at BS along with the Rake receiver and the Pre-Rake transmitter to achieve a processing gain for suppressing multiple access interference. The system concept is demonstrated by computer simulations. In addition, the associated transceiver architecture and a TDD time slot structure are presented for practical system concerns. Moreover, it is shown through analysis that the total average data throughput equals 3.8 Gbps and the system can achieve a bandwidth efficiency of 19 bps/Hz/cell on 200 MHz transmission bandwidth.**

***Keyword*—5G communication, cellular system, massive antennas, millimeter wave, TDD**

I. Introduction

Recently, many studies have sprung up in the world [1]-[8] for 5G systems. According to the IMT-2020 released in 2015 [9], stringent system requirements are specified for future 5G systems. On the link level and system level, the next generation 5G mobile radio communication system demands both the high data rate and high system capacity.

Potential technologies for the future 5G system are in the scope of heterogeneous networks, millimeter wave (mmWave) transmission, and massive multiple-input multiple-output (massive MIMO) antennas [8]. The first scheme basically evolves from the Long Term Evolution (LTE) and allows different kinds of cells to function and cooperate in the same geographical area. The second scheme makes use of the unexplored spectrum in the millimeter wave band since it not only avoids frequency spectrum congestion problem below 6 GHz but also provides enough bandwidth for high data rate transmission. Nevertheless, it leads to the inherent problem of much larger propagation loss in much higher frequency bands. The third approach considered employs a large amount of antennas at BS side [10]-[16], usually tens to hundreds of antennas, that offers substantial degrees of freedom for baseband signal processing. Combining millimeter wave transmission with the massive antennas at BS side, this paper presents a multipath division multiple access (MDMA) [17] time division duplexing (TDD) cellular system that is able to provide both the high data rate and high system capacity.

Contributions of this article are briefed in the following. A novel cellular system built upon MDMA for the 5G mobile communication is proposed. In the uplink (UL), MDMA distinguishes its users by exploiting their distinct multipath characteristics through employing RAKE receivers with massive antennas at BS. Similarly, the Pre-RAKE precoding technique with massive antennas is adopted at BS in the downlink (DL). Moreover, every user terminal (UT) is equipped with single antenna that greatly alleviates the signal processing burden. It is shown in Section III that both system capacity and the aggregated data rate can be boosted up to an appreciable extent. Thus, the proposed MDMA TDD cellular system is a promising candidate for future 5G systems.

The paper is organized as follows. Section II gives the radio system architecture, including the transceiver architecture, the associated time slot structure, and a simplified analysis. Section III uses computer simulations as an auxiliary method to illustrate the system concept and provides a simplified analysis to verify the performance of the MDMA system. Finally, the paper completes with conclusions in Section IV.

II. System Architecture

The proposed MDMA cellular system layout is shown in Fig. 1, which operates on the premise of the following assumptions.

1) The system exploits massive antennas operating in the mmWave band, e.g., 30GHz, such that the size of each antenna (e.g., dipole antenna) is very small.
2) The BS antennas are separated by every other 10 wavelengths (at least) to make their received signals nearly uncorrelated [18]. For example, if we arrange 100 antennas in a two-dimensional square grid, then the total

Manuscript received October 24, 2016. This work is a follow-up of the invited journal to an accepted out-standing conference paper of the 18th International Conference on Advanced Communication Technology (ICACT 2016). This research is supported by the Ministry of Science and Technology (MOST) of R.O.C.

W. H. Hsiao is with the Department of Electrical and Computer Engineering, National Chiao Tung University, No.1001, Daxue Rd., East Dist., Hsinchu City 300, Taiwan (R.O.C.) (Corresponding author, Phone: +886-3-5712121 ext. 54579; e-mail: whsiao.cm97g@g2.nctu.edu.tw).

C. C. Huang is with the Department of Electrical and Computer Engineering, National Chiao Tung University, No.1001, Daxue Rd., East Dist., Hsinchu City 300, Taiwan (R.O.C.) (e-mail: huangcc@faculty.nctu.edu.tw).

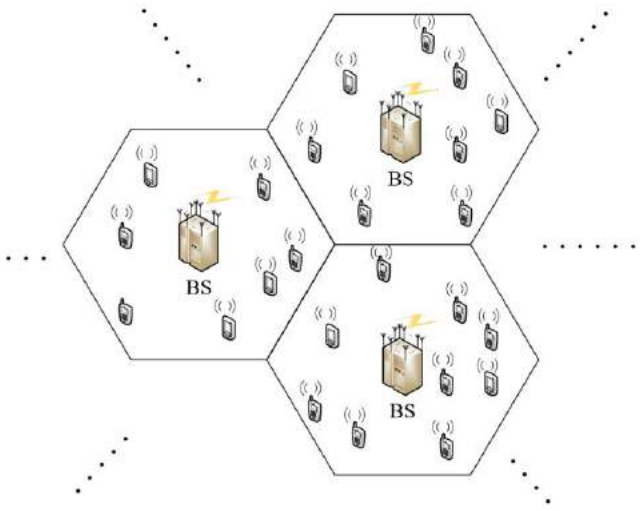

Fig. 1. The proposed MDMA 5G cellular system layout.

area occupied is about 1 m^2, which can be easily deployed in real environments.

3) Channel bandwidth of 200 MHz is assumed in our system. With such wideband transmission, the rich and distinct multipath components of each individual user can be resolved, which helps to distinguish all the users.
4) Time division duplexing (TDD) is adopted here, thus we assume channel reciprocity in uplink and downlink transmissions.
5) UL channel state information (CSI) is known at BS through channel estimation, which can also be used for precoding in DL transmission.
6) Power control is executed in the uplink, i.e., the received power level of each user at BS is nearly equal.
7) A UT is always served by the base station that provides it with the largest received power level.
8) The proposed cellular system is interference limited, i.e., the background noise can be ignored as compared with the interferences.

The equalization of the channel is done in both time and space domains via the Rake receiver and Pre-Rake [19] transmitter in the uplink and downlink, respectively. This leads to a huge signal-to-interference plus noise ratio (SINR) gain for each user when massive antennas are used in the BS. The resultant spatial processing gain is analogous to a CDMA system's processing gain and is effective in suppressing intersymbol interference (ISI), multiple access interference (MAI), and cochannel interference (CCI).

A. Uplink Transceiver Architecture

Fig. 2(a) shows the block diagram of the uplink MDMA transceiver [17]. Consider a multi-user scenario with K single-antenna users and an M-antenna BS in each cell. Assume the binary phase shift keying (BPSK) modulation is used. Then the transmit data bit stream of user k can be written as

$$s_k^{\mathrm{u}}(t) = \sum_n s_k^{\mathrm{u}}(n)\delta(t - nT_b)\ ,\quad k = 1,2,...K\ , \tag{1}$$

where the superscript u, $\delta(\cdot)$, and T_b denote the uplink transmission, the Dirac delta function, and the bit time, respectively. Assume the transmit power $\mathbf{E}\left|s_k^{\mathrm{u}}(t)\right|^2 = 1$ for simplicity, where $\mathbf{E}$ is the expectation operator.

The multipath channel between the kth user and the j-th BS antenna is

$$h_{kj}(t) = \sum_{l=1}^{L} \alpha_{lkj}\delta(t - \tau_{lkj})\ ,\quad k = 1,2,...K.\ j = 1,2,...M\ , \tag{2}$$

where α_{lkj} and τ_{lkj} represent the complex gain and the delay of the l-th path. For normalization, we assume the power gain $\sum_{l=1}^{L}\mathbf{E}\left|\alpha_{lkj}\right|^2 = 1$.

Thus, the received signal at the j-th BS antenna from the k-th user reads

$$\begin{aligned} v_{kj}(t) &= \sum_{l=1}^{L}\sum_n \alpha_{lkj}\, p(t - \tau_{lkj} - nT_b)s_k^{\mathrm{u}}(n) \\ &= s_k^{\mathrm{u}}(t) \otimes p(t) \otimes h_{kj}(t)\ , \end{aligned} \tag{3}$$

where $p(t)$ is the impulse response of the transmit filter with $\int_{-\infty}^{\infty} p^2(t)\,dt = 1$ and $\otimes$ denotes the linear convolution operator.

Hence, the output of the k-th user's Rake receiver at the j-th BS antenna equals to

$$\begin{aligned} u_{kj}(t) &= \left(v_{kj}(t) + \sum_{\substack{q=1 \\ q\neq k}}^{K} v_{qj}(t) + \mathrm{CCI} + n_j(t) \right) \\ &\quad \otimes \sum_{l'=1}^{L} \alpha_{l'kj}^{*}\, p^{*}(-t - \tau_{l'kj}) \\ &= \left(\begin{array}{l} s_k^{\mathrm{u}}(t) \otimes p(t) \otimes h_{kj}(t) + \sum\limits_{\substack{q=1 \\ q\neq k}}^{K} s_q^{\mathrm{u}}(t) \otimes p(t) \otimes h_{qj}(t) \\ + \mathrm{CCI} + n_j(t) \end{array} \right) \\ &\quad \otimes p^{*}(-t) \otimes h_{kj}^{*}(-t)\ , \end{aligned} \tag{4}$$

where $n_j(t)$ is the additive white Gaussian noise at the j-th BS antenna and the cochannel interference (CCI) comes from other cells. Note that the Rake receiver here is represented by $p^{*}(-t) \otimes h_{kj}^{*}(-t)$, where $*$ denotes the complex conjugation.

Finally, the BS detects the n-th data bit of user k according to the decision metric $\sum_{j=1}^{M} u_{kj}(t)$ at $t = nT_b$.

B. Downlink Transceiver Architecture

Fig. 2(b) shows the corresponding block diagram of the downlink transceiver. The data bit stream of each user is precoded by the Pre-Rake transmitter for each BS antenna. Meanwhile, the required CSI is obtained through uplink channel estimation and it is used for Pre-Rake precoding. It is worth noting that the Pre-Rake precoding moves the equalization effort to the BS transmitter that helps to reduce the complexity of the UT receiver.

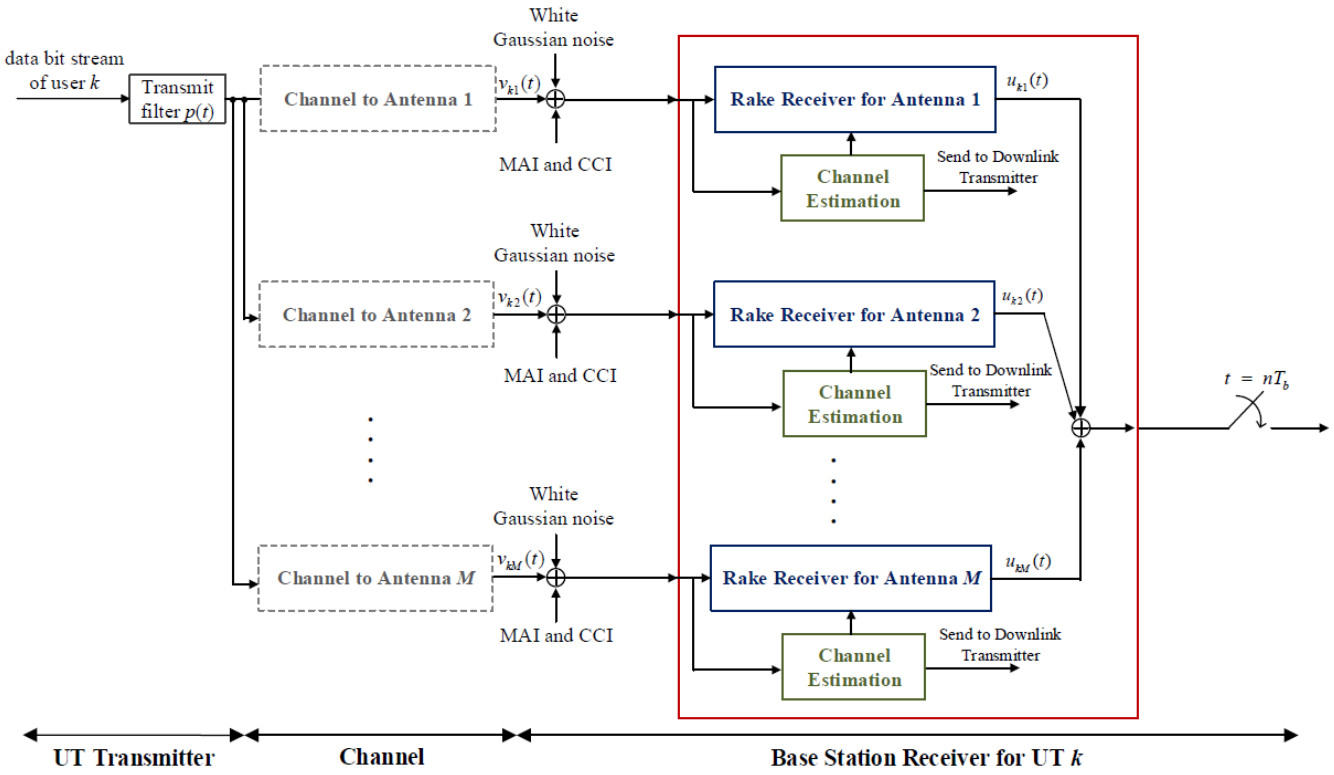

(a)

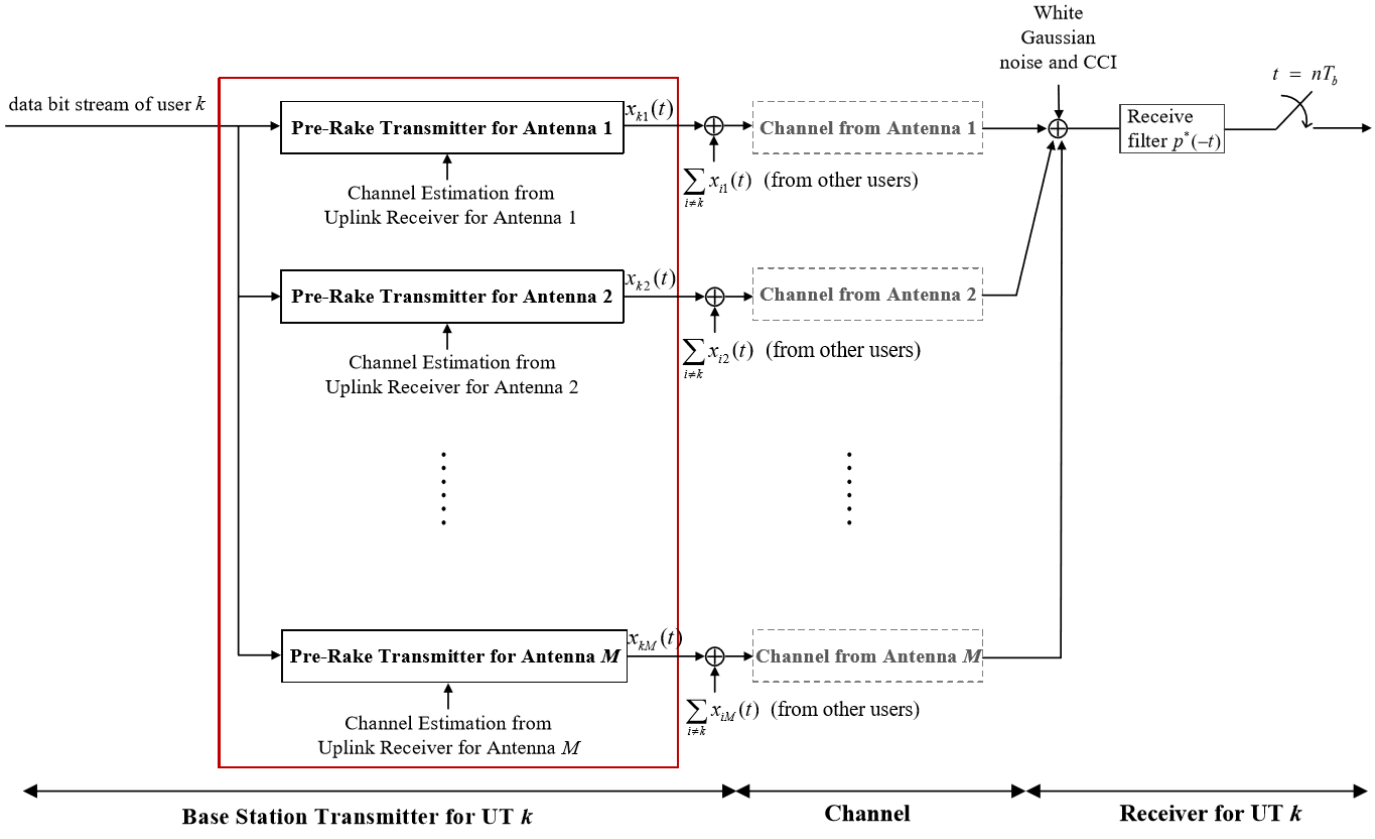

(b)

Fig. 2. MDMA transceiver architecture for (a) uplink and (b) downlink.

The output of the user k's Pre-Rake transmitter for antenna j is

$$x_{kj}(t) = s_k^{\mathrm{d}}(t) \otimes p^*(-t) \otimes h_{kj}^*(-t) = \sum_{l=1}^{L} \sum_{n} \alpha_{lkj}^* p^*(t + \tau_{lkj} - nT_b) s_k^{\mathrm{d}}(n) , \quad (5)$$

where the superscript d denotes the downlink transmission.

Thus, the transmitted signal at the j-th antenna is $\sum_{k=1}^{K} x_{kj}(t)$, i.e., the sum over all the users' Pre-Rake transmitter outputs for the j-th BS antenna.

In the user terminal, the data is detected by sampling the received signal at the correct sampling time and making decisions accordingly.

C. Simplified Analysis

An analysis of the single cell scenario is considered here from link level point of view while the multi-cell scenario is discussed in Section III from system capacity point of view.

Since the Rake reception and the Pre-Rake transmission provide the same signal-to noise ratio (SNR) as proved in [19] for single BS antenna case, we only show here the uplink SIR performance of the system with massive antennas at BS.

Assume user k represents the desired user. Insert (3) into (4) and neglect MAI, CCI and noise terms for now, we get

$$u_{kj}(t) = \int_{-\infty}^{\infty} \left(\sum_{l=1}^{L} \sum_{m} \alpha_{lkj} p(\lambda - \tau_{lkj} - mT_b) s_k(m) \right) \times \left(\sum_{l'=1}^{L} \alpha_{l'kj}^* p^*(-t + \lambda - \tau_{l'kj}) \right) d\lambda . \quad (6)$$

Here, we use a bandlimited filter $p(t) = \frac{1}{\sqrt{T_b}} \mathrm{sinc}\left(\frac{t}{T_b}\right)$ since it satisfies not only $\int_{-\infty}^{\infty} p^2(t)\, dt = 1$ but also the Nyquist criterion, i.e., $p_{eff}(iT_b) = \delta[i]$, $i \in \mathbb{Z}$, where $\delta[n]$ is the Kronecker delta function and $p_{eff}(t) \equiv p(t) \otimes p^*(-t)$.

Thus, sampling (6) at $t = nT_b$ results in

$$\begin{aligned} u_{kj}(nT_b) &= \int_{-\infty}^{\infty} \left(\sum_{l=1}^{L} \sum_{m} \alpha_{lkj} p(\lambda - \tau_{lkj} - mT_b) s_k^{\mathrm{u}}(m) \right) \times \left(\sum_{l'=1}^{L} \alpha_{l'kj}^* p^*(-nT_b + \lambda - \tau_{l'kj}) \right) d\lambda \\ &= \int_{-\infty}^{\infty} \left(\sum_{l=1}^{L} |\alpha_{lkj}|^2 p^2(\lambda - \tau_{lkj} - nT_b) s_k^{\mathrm{u}}(n) \right) d\lambda + \mathrm{ISI} \\ &= s_k^{\mathrm{u}}(n) + \mathrm{ISI} . \end{aligned} \quad (7)$$

The last equality holds due to wideband transmission, say 200 MHz in our system. That is, $\sum_{l=1}^{L} |\alpha_{lkj}|^2 \cong \sum_{l=1}^{L} \mathbf{E}|\alpha_{lkj}|^2 = 1$ for large L. Combine *coherently* all the Rake receiver's outputs and sample at time nT_b for user k, one can get the desired signal as $Ms_k^{\mathrm{u}}(n)$, i.e., the desired signal power becomes M^2 times of that in the single-antenna case.

Since the interference mainly comes from other users in the same cell, i.e., MAI can be modeled as

$$z_k(t) = \sum_{j=1}^{M} \sum_{q \neq k} s_q^{\mathrm{u}}(t) \otimes p(t) \otimes h_{qj}(t) \otimes h_{kj}^*(-t) \otimes p^*(-t) = \sum_{j=1}^{M} \sum_{q \neq k} s_q^{\mathrm{u}}(t) \otimes \left[p(t) \otimes p^*(-t) \right] \otimes h_{qj}(t) \otimes h_{kj}^*(-t) = \sum_{j=1}^{M} \sum_{q \neq k} s_q^{\mathrm{u}}(t) \otimes p_{eff}(t) \otimes h_{qj}(t) \otimes h_{kj}^*(-t) . \quad (8)$$

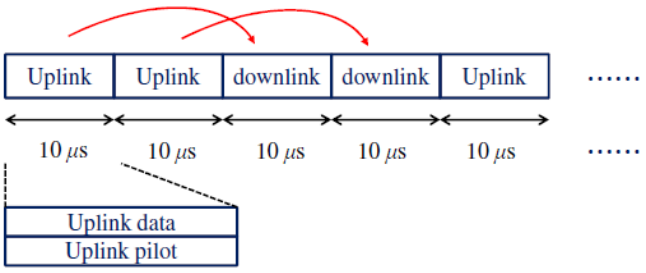

Fig. 3. The proposed time slot structure

Due to the channel's randomness and normalization among all users, the interference power from MAI in (8) can be calculated as $M(K-1)$ according to [23, p.5]. Note that we assume the channel has unit power gain. In fact, the result is a direct consequence of the *noncoherent* addition of the interference terms over all receive BS antennas.

We can easily calculate the equivalent E_b/I_0 of each user and the result is approximately equal to M/K when M is large. Since massive antennas are used at BS, the equivalent E_b/I_0 could be boosted up to a required amount. In other words, the end-to-end equivalent channel of each user gradually approaches an ideal channel, an impulse-like channel, when M is large. Thus, M is the processing gain which can be offered by the MDMA cellular system. Similarly, an equal amount of processing gain can be achieved for each DL user through Pre-RAKE precoding.

D. Time Slot Structure

Since the channel coherence time at a carrier frequency of 1 GHz and a vehicle speed of 100 km/hr is roughly 600 μs[1] [20], the corresponding coherence time at 30 GHz is about 20 μs, because it is inversely proportional to the carrier frequency. Therefore, the system we considered needs to estimate the channel with a time period of 20 μs. Fig. 3 shows the time slot structure of the TDD cellular system. A time slot (TS) duration of 10μs amounts to 2000 bits for both UL and DL. Two DL time slots directly follow two UL time slots. Together with the data signal, the UL time slots also transmit a pilot signal with the same power level as the data signal for the purpose of channel estimation. Furthermore, a 10 μs processing time is reserved such that the channel estimation result in the first UL TS can be used for the first DL TS while the second UL TS channel estimation result is used for the second DL TS, as the red arrows point out in Fig. 3. Although this pilot-added approach inevitably causes extra interference for UL data detection, advanced signal processing techniques such as iterative cancellation can be applied to reduce the interference effect. The relevant channel estimation and interference cancellation techniques, out of the scope of this article, are treated in another paper.

[1] Recall that the packet duration in GSM is 577 μs, in this time period the channel can be regarded as quasi-static at a vehicle speed of 100 km/hr in 1 GHz band [20].

III. Computer simulation and system capacity evaluation

In the computer simulations which are used to illustrate the MDMA cellular system concept, we modify the S-V channel model according to the spatial parameters given in [21]. First, we generate the number of clusters by the Poisson distribution. Then, the arrival time of the different clusters is set to be uniformly distributed within the maximum delay spread, e.g., 404.1 ns [22]. Second, we calculate the power of each cluster using the model of [21]. Third, we generate the inter-arrival time of each ray within individual cluster according to the exponential distribution. Finally, we calculate the power of each ray. In addition, the time resolution of multipath in our 5G system is equal to 5 ns (due to 200 MHz channel bandwidth), which is the same as the time resolution in the original S-V model. Thus, the path delay is quantized to the nearest integer multiple of 5 ns. Note that a ray will be dropped when its power is less than a predefined threshold, e.g., 10 dB below the strongest path. A realization of the channel impulse response is plotted in Fig. 4.

Fig. 5 shows an effective end-to-end channel of a desired user in a single cell which serves 25 users simultaneously. The effective end-to-end channel of user k is defined here as the discrete-time version of $\sum_{j=1}^{M}\sum_{q=1}^{K} h_{qj}(t) \otimes h_{kj}^{*}(-t)$. It is apparent that as the number of BS antennas increases, the interferences get more suppressed relative to the desired signal, which agrees with the simplified analysis in Section II C when M grows large. That is, the interferences including MAI and ISI can be suppressed with a large number of BS antennas. Moreover, the power of the desired signal is nearly M^2 times as expected.

Fig. 6 plots the cumulative distribution of the uplink receive SIR with 100 BS antennas and different number of users in a *multi-cell* scenario. In the simulations, the cellular system is constructed with 127 hexagonal cells (each with a radius of 250 m) which include 6 tiers of cochannel cells. For simplicity, assume uplink channel is known at BS in advance. Some observations can be made here. First, it can be observed that the mean of receive SIR is proportional to M / K which matches the simplified analysis result in the previous section. Similarly, the SIR distribution gets improved as the ratio of M / K increases. On one hand, the mean of the receive SIR is less than M / K by a factor of $2 / 3$ (-1.7 dB) which is caused by all the other cell interference. On the other hand, variations around the mean of the receive SIR diminish as the number of users increases due to the law of large numbers. That is, the receive SIR converges to its mean as more users are served in the system. Fig. 7 plots the cumulative distribution of the downlink receive SIR. Again, it reveals that the mean of receive SIR is proportional to M / K as in the downlink. However, the receive SIR distribution is worse than the uplink case since higher tail probability can be observed. This is because there is no power control in the downlink, which causes more serious cochannel interference problems.

Here, we define $f_{99\%}$ to be the other-cell relative interference factor for the worst 1% in the SIR cumulative distribution functions, i.e., the probability that the SIR value exceeds a predefined SIR threshold is greater than 0.99. In [24], $f_{99\%}$ is found to be 0.7 in the uplink with power control, while it is relatively larger and is about 3.6 in the downlink without power control. By examining the initial portion of Fig. 6 and Fig. 7 closely, we found these values ($f_{99\%} = 0.7$ or 3.6) are consistent with our simulation results with hexagonal cell layout, such that they are applied here.

Toward the MDMA TDD cellular system, a simple evaluation of its system capacity is given here. Recall that the system considered operates in the carrier frequency of 30 GHz with a channel bandwidth of 200 MHz, and has a frequency reuse factor of one. Also note that K and M are the number of users in a cell and the number of BS antennas respectively. Assume BPSK modulation and ideal power control in the uplink. In the worst case, the system is in full loading, i.e., K users are transmitting concurrently. In this situation, the SIR at each user's demodulator output is thus

$$\frac{E_b}{I_0} \cong \frac{S}{I} = \frac{M^2}{M(K-1)} \times \frac{1}{1+f_{99\%}} = \frac{M}{K-1} \times \frac{1}{1+f_{99\%}}, \tag{9}$$

where E_b and I_0 represent the received energy per bit and the interference power spectrum density. S and I are respectively the average signal power and interference power. $\frac{M^2}{M(K-1)}$ comes from the fact that the desired signal of each BS antenna adds coherently while the interference sums up noncoherently.

Rearranging (9) leads to

$$K \cong \frac{M}{E_b/I_0} \times \frac{1}{1+f_{99\%}}, \tag{10}$$

which gives an elegant formula to calculate the number of users the BS can serve under the required E_b / I_0 at each user's demodulator output.

We consider first data transmission in the uplink time slots as described in Section II with half power allotted to data and pilots. Assume a minimum E_b / I_0 of 6 dB for data detection that provides the acceptable performance [23, pp.8], 300 BS antennas can serve 22 full loaded users in every cell simultaneously, since $\frac{300}{4} \times \frac{1}{1+0.7} \times \frac{1}{2} \cong 22$, where the last one-half factor counts for the reduction in SIR due to uplink pilots. Now we consider transmission in the downlink time slots. Since there are no pilots used in the downlink, the total number of simultaneous users which can be served turns out to be $\frac{300}{4} \times \frac{1}{1+3.6} \cong 16$. In a real system, the number of simultaneous users can be greatly increased if they are not full loaded.

Since each user in the cell shares the whole 200 MHz bandwidth, the proposed TDD cellular system can at least provide a total average data throughput of 200 Mbps $\times$ $(22+16)\times\frac{1}{2} = 3.8$ Gbps. Thus, the system achieves a bandwidth efficiency of 19 bps/Hz/cell.

Note that the system capacity can be further enhanced if multi-user detection techniques (e.g., successive interference cancellation or parallel interference cancellation) are used to eliminate intra-cell interference. The system capacity can be increased since the factor $1 / (1+f_{99\%})$ in (10) could be replaced by $1 / f_{99\%}$ if the intra-cell interference can be totally cancelled.

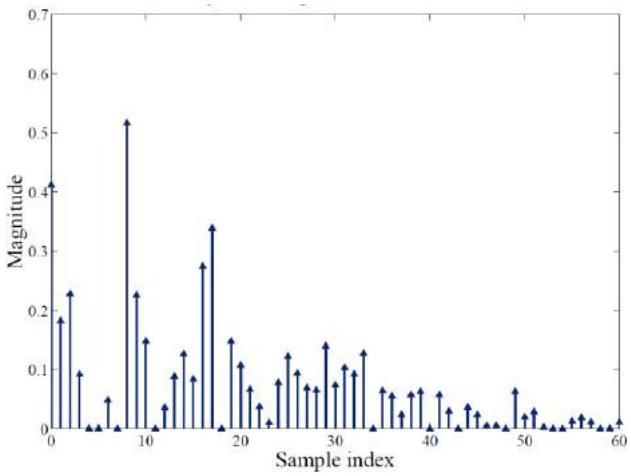

Fig. 4. A realization of the channel amplitude response.

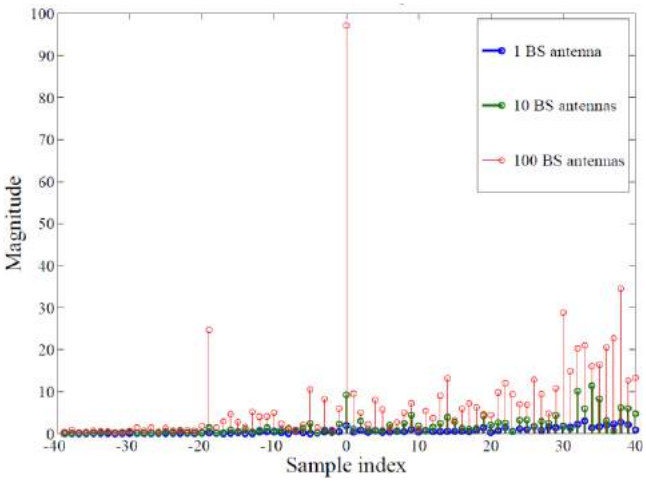

Fig. 5. An effective end-to-end channel of a desired user in a full loading cell with 25 active users.

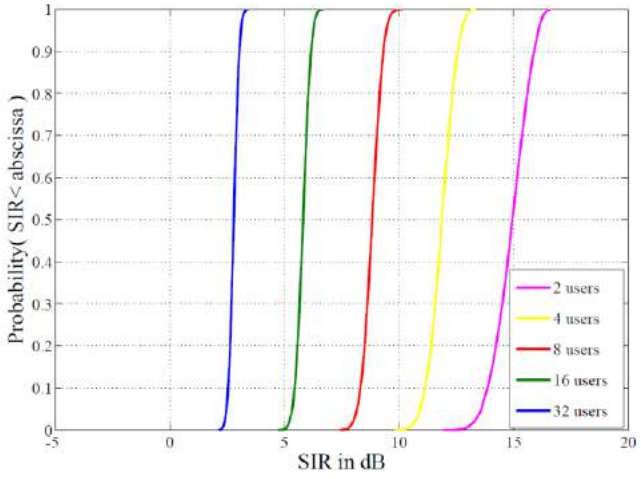

Fig. 6. The cumulative distribution of the uplink receive SIR with 100 BS antennas and different number of active users in a multi-cell scenario.

IV. Conclusion

The next generation (5G) cellular communication system demands both high system capacity and high data rate. A novel cellular system architecture built upon MDMA is proposed for the future 5G cellular mobile communication. MDMA is a multiple access method to use massive antennas at BS together with the Rake receiver and the Pre-Rake

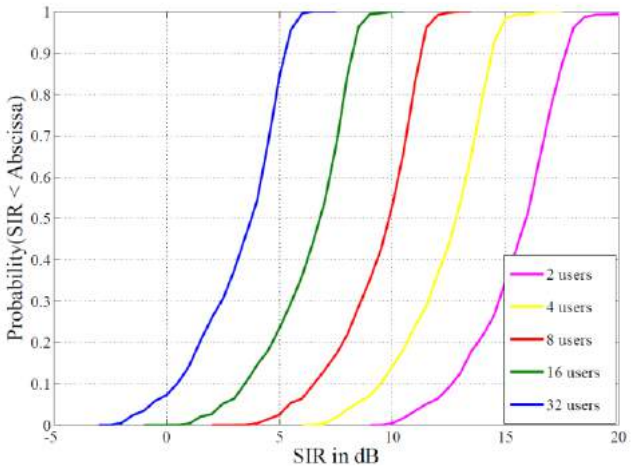

Fig. 7. The cumulative distribution of the downlink receive SIR with 100 BS antennas and different number of active users in a multi-cell scenario.

transmitter to achieve a processing gain to suppress multiple access interference in a TDD cellular mobile radio system. The transceiver architecture and the TDD time slot structure are described in the article. On the other hand, the user terminal is kept simple because only single antenna is used for every user. From simulations and simple analysis, it is shown that both system capacity and aggregated data throughput can be boosted up to a considerable level for a cellular system with a frequency reuse factor of one. The system can serve on average 19 ($=(22+16)\times 0.5$) users in each cell with the total average data throughput of 3.8 Gbps on 200 MHz transmission bandwidth which achieves a bandwidth efficiency of 19 bps/Hz/cell. In brief, the proposed MDMA TDD cellular system can serve as a candidate system architecture for future 5G wireless communication.

References

[1] METIS website. (2015) [Online]. Available: https://www.metis2020.com

[2] European Commission. (2013). 5GNOW-5th Generation Non-Orthogonal Waveforms for Asynchronous Signaling. [Online]. Available: http://cordis.europa.eu/fp7/ict/future-networks/documents/call8-projects/5gnowfactsheet.pdf

[3] Alcatel-Lucent. (2011). LTE and beyond, [Online]. Available: http://web.dit.upm.es/~doct/SI/2011-2012

[4] NTT DOCOMO, "Future Radio Access for 5G", white paper, Jul. 2014

[5] W. Roh. (2013). Performances and Feasibility of mmWave Beamforming Prototype for 5G Cellular Communications. Presented at IEEE ICC. [Online]. Available: http://www.faculty.poly.edu/~tsr

[6] G. Wunder *et al*., "5GNOW: Challenging the LTE Design Paradigms of Orthogonality and Synchronicity," *2013 IEEE 77th Vehicular Technology Conference (VTC)*, Jun. 2013.

[7] A. Osseiran *et al.*, "The foundation of the mobile and wireless communications system for 2020 and beyond: challenges, enablers and technology solutions," *2013 IEEE 77th Vehicular Technology Conference (VTC)*, Jun. 2013.

[8] J. G. Andrews *et al.*, "What will 5G be?," *IEEE Journal on Sel. Areas in Communications*, vol. 32, no. 6, pp. 1065−1082, Jun. 2014.

[9] ITU website. (2015) [Online]. Available: http://www.itu.int/en

[10] T. L. Marzetta, "Noncooperative cellular wireless with unlimited numbers of base station antennas," *IEEE Trans. on Wireless Communications*, vol. 9, no. 11, pp. 3590−3600, Nov. 2010.

[11] A. Pitarokoilis, S. K. Mohammed, and E.G. Larsson, "On the optimality of single-carrier transmission in large-scale antenna systems," *IEEE Wireless Communications Letters*, vol. 1, no. 4, pp. 276−279, Aug. 2012.

[12] J. Hoydis, S. ten Brink, and M. Debbah, "Comparison of linear

precoding schemes for downlink massive MIMO," *2012 IEEE International Conference on Communications (ICC)*, pp. 2135–2139, Jun. 2012.
[13] F. Rusek *et al*., "Scaling up MIMO: opportunities and challenges with very large arrays," *IEEE Signal Processing Magazine*, vol. 30, no. 1, pp. 40–60, Jan. 2013.
[14] J. Zhang *et al*., "On capacity of large-scale MIMO multiple access channels with distributed sets of correlated antennas," *IEEE Journal on Sel. Areas in Communications*, vol. 31, no. 2, pp. 133–148, Feb. 2013.
[15] J. Hoydis, S. ten Brink, and M. Debbah, "Massive MIMO in the UL/DL of cellular networks: how many antennas do we need?," *IEEE Journal on Sel. Areas in Communications*, vol. 31, no. 2, pp. 160–171, Feb. 2013.
[16] E. Larsson *et al*., "Massive MIMO for next generation wireless systems," *IEEE Communications Magazine*, vol. 52, no. 2, pp. 186–195, Feb. 2014.
[17] W. H. Hsiao and C. C. Huang, "Multipath division multiple access for 5G cellular system based on massive antennas in millimeter wave band," the *18th Intl. Conf. on Advanced Communications Technology (ICACT)*, pp.741–746, Jan. 2016.
[18] C. Y. Lee, "Mobile radio performance for a two-branch equal-gain combining receiver with correlated signals at the land site," *IEEE Trans. on Vehicular Technology*, vol. 27, no. 4, pp. 239–243, Nov. 1978.
[19] R. Esmailzadeh and M. Nakagawa, "Pre-RAKE diversity combination for direct sequence spread spectrum mobile communications systems," *IEICE Trans. Communications.*, vol. E76-B, no. 8, pp. 1008–1014, Aug. 1993.
[20] T. S. Rappaport, *Wireless Communications: Principles and Practice*, 2nd ed., Prentice Hall, 2002.
[21] M. R. Akdeniz, Y. Liu, S. Sun, S. Rangan, T. S. Rappaport, and E. Erkip, "Millimeter wave channel modeling and cellular capacity evaluation," *IEEE Journal on Sel. Areas in Communications*, Sep. 2014.
[22] S. Sun and T. S. Rappaport, "Multi-beam antenna combining for 28 GHz cellular link improvement in urban environments," in *Proc. IEEE Globecom*, Dec. 2013.
[23] A. J. Viterbi, *CDMA: Principles of Spread Spectrum Communication*, Prentice Hall, 1995.
[24] C. C. Huang, "Computer simulation of a direct sequence spread spectrum cellular radio architecture," *IEEE Trans. on Vehicular Technology*, vol. 41, no. 4, pp. 544–550, Nov. 1992.

Wei-Han Hsiao was born in Taiwan, R.O.C. He received the B.S. degree in electrical and control engineering from National Chiao Tung University (NCTU), Hsinchu, Taiwan, in 2008. He is currently pursuing the Ph.D. degree in communications engineering since 2010 in NCTU. His current research interests are on transceiver design and analysis for next generation mobile communication systems**.**

Chia-Chi Huang was born in Taiwan, R.O.C. He received the B.S. degree in electrical engineering from National Taiwan University in 1977 and the M.S. and Ph.D. degrees in electrical engineering from the University of California, Berkeley, in 1980 and 1984, respectively.

From 1984 to 1988, he was an RF and communication system engineer with the Corporate Research and Development Center, General Electric Company, Schenectady, NY, where he worked on mobile radio communication system design. From 1989 to 1992, he was with the IBM T.J. Watson Research Center, Yorktown Heights, NY, as a Research Staff Member, working on indoor radio communication system design. Since 1992, he has been with National Chiao Tung University, Hsinchu, Taiwan, and currently as Professor in the Department of Electrical and Computer Engineering. His research areas are in mobile radio, wireless communication, and cellular systems.